Plasma Reconfigurable Frequency Selective Surfaces

Theodore anderson
Haleakala Research and Development, Inc, 7 Martin Road, Brookfield, MA., 01506, USA , tedanderson@haleakala-research.com

Abstract— Plasma frequency selective surfaces (FSS) use plasma instead of metal for the FSS elements. Frequency selective surfaces have been used for filtering electromagnetic waves. In conventional metal FSS, each layer has to be modeled using numerical methods and the layers are stacked in such a way to create the desired filtering. Genetic algorithms are sometimes used to determine the stacking needed for the desired filtering. This is a complicated and numerically expensive process. The plasma frequency selective surfaces can be tuned to a desired filtering by varying any or all of the density, size, shape, and spacing of the plasma elements.

***Index Terms*— frequency selective surfaces, measurement, plasma, reconfigurable.**

I. INTRODUCTION

Theorectical and experimental work on plasma frequency selective surfaces has been done Anderson and Alexeff [1]. Anderson [2] has a book chapter on plasma frequency selective surfaces. Munk [3] wrote a comprehensive book on conventional frequency selective surfaces using metal. As the density of the plasma is increased, the plasma skin depth becomes smaller and smaller until the elements behave as metallic elements and we create filtering similar to FSS with metallic elements. Up until the metallic mode for the plasma, our theory and experiments showed that the plasma FSS had a continuous change in filtering. A basic mathematical model for a plasma FSS is developed by modeling the plasma elements as half wavelength and full wavelength dipole elements in a periodic array on a dielectric substrate. The theoretical model with numerical predictions predicted results in good agreement with our experiments on the plasma FSS. Theoretically Floquets Theorem is used to connect the elements. The transmission and reflection characteristics of the plasma FSS as a function of plasma density is developed. Frequencies from around 900 MHz to 12 GHz are utilized with a plasma density around 2 GHz. was transparent. Corresponding work on plasma antennas can be found in [4] – [5]. Plasma is a type of metamaterial [6] and can be treated as such in plasma FSS and plasma antennas.

II. PLASMA FSS THEORY

A. Selecting a Template (Heading 2)

An FSS dipole array consists of a periodic array of vertically aligned scattering elements. In traditional FSS structures, the scattering elements would be made of some material possessing good electrical conductivity (and thus high reflectivity).

For a plasma FSS structure, we imagine a scattering element to consist of gaseous plasma contained in a tube. The purpose of the present investigation is to determine the electromagnetic scattering properties of the array as a function of the reflectivity of the plasma elements.

B. Method of calculation

The response (reflection and transmission) of the plasma FSS is calculated in two stages. (1) The response for a perfectly conducting structure is given. (2) Then we scale the reflectivity by a function that depends on the incident frequency and the plasma frequency so as to account for the scattering properties of the plasma. Details of these two steps will now be presented.

C. Periodic Moment Method

In the first stage of calculation, we use the Periodic Moment Method s described in the book by Munk [3]. The elements are approximated as thin flat wires. The scattered electric field produced by an incident plane wave of a single frequency is given by:

$$\bar{E}(\bar{R}) = -I_A \frac{Z}{2D_x D_y} \sum_{k=-\infty}^{\infty} \sum_{n=-\infty}^{\infty} \frac{e^{-j\beta \bar{R} \bullet \hat{r}_{\pm}}}{r_y} [(_{\perp}\hat{n}_{\pm})(_{\perp}P) + (_{\parallel}\hat{n}_{\pm})(_{\parallel}P)]. \quad (1)$$

The quantities in this equation are defined as follows. The quantity I_A is the current induced in a single element by the incident plane wave (see Munk [3]), Z is the impedance of the medium which we take to be free space ($Z = 377\Omega$) , $\bar{R}$ is the position vector of the observation point, and the scattering vector is defined by:

$$\hat{r}_{\pm} = \hat{x} r_x \pm \hat{y} r_y + \hat{z} r_z \,, \quad (2)$$

with,

$$r_x = s_x + k\frac{\lambda}{D_x} \,,\; r_z = s_z + n\frac{\lambda}{D_z} \quad (3)$$

and,

$$r_y = \sqrt{1 - (s_x + k\frac{\lambda}{D_x})^2 - (s_z + n\frac{\lambda}{D_z})^2} \quad (4)$$

In these equations, s_x, and s_z, are the components of the

unit vector specifying direction of the incident plane wave. The array is assumed to lie in the x-z plane with repeat distances D_x, and D_z, and the directions $\pm\hat{y}$ indicate the forward and back scattering directions respectively. Note that for sufficiently high values of the integers, n and k, the scattering vector component r_y becomes imaginary corresponding to evanescent modes.

The remaining quantities (in the square brackets of the expression for the scattered field) are related to the way in which the incident electric field generates a voltage in an array element as is described in detail in Munk [2], The voltage induced in a scattering element by the incident field is given by:

$$V(\bar{R}) = \bar{E}(\bar{R}) \bullet \hat{p}P, \tag{5}$$

where, $\bar{E}(\bar{R})$ is the electric field vector of the incident plane wave, $\hat{p}$ is a unit vector describing the orientation of the scattering element, and P is the pattern function for the scattering element and is defined by:

$$P = \frac{1}{I^t(\bar{R})} \int_{Element} I^t(l) e^{-j\beta l \hat{p} \bullet \hat{s}} dl, \tag{6}$$

where, $I^t(l)$, is the current distribution on the element located at $\bar{R}$, $I^t(\bar{R})$ is the current at the terminals of the scattering element (e.g. at the center of a dipole antenna), $\hat{s}$ is the unit vector denoting the plane wave incident direction, and $\beta = 2\pi/\lambda$ is the wave number. The unit vectors ${}_{\perp}\hat{n}$ and ${}_{\parallel}\hat{n}$, which describe the electric field polarization, are defined by:

$${}_{\perp}\hat{n} = \frac{-\hat{x}r_z + \hat{z}r_x}{\sqrt{r_x^2 + r_z^2}}, \tag{7}$$

and,

$${}_{\parallel}\hat{n} = {}_{\perp}\hat{n} \times \hat{r} = \frac{1}{\sqrt{r_x^2 + r_z^2}} \left[-\hat{x}r_x r_y + \hat{y}(r_x^2 + r_z^2) - \hat{z}r_y r_z \right] \tag{8}$$

The quantities ${}_{\perp}P$, and ${}_{\parallel}P$, are given by multiplying the pattern function by the appropriate direction cosine: ${}_{\perp}P = \hat{p} \bullet {}_{\perp}\hat{n}P$, and ${}_{\parallel}P = \hat{p} \bullet {}_{\parallel}\hat{n}P$. The effective terminal current I_A which enters the equation for the scattered electric field is obtained from the induced voltage and the impedance as:

$$I_A = \frac{V}{Z_A + Z_L}, \tag{9}$$

where, Z_L is the self-impedance of the scattering element, and Z_A is the impedance of the array.

As in all moment methods, some approximation must be made regarding the detailed current distribution on the scattering elements. In order to calculate the pattern function, we assume the current distribution to be a superposition of current modes. The lowest order mode is taken to be a sinusoidal distribution of the form:

$$I_0(z) = \cos(\pi z / l) \tag{10}$$

Where assuming the scattering element to be a conductor of length l centered at the origin. Thus the lowest order mode corresponds to an oscillating current distribution of wavelength $\lambda = 2l$. This lowest order mode gives rise to a radiation pattern equivalent to a dipole antenna with a current source at the center of the dipole. In effect, this mode divides the scattering elements of Figure27 into two segments. The next two higher order modes are constructed by dividing each half of the scattering element into two more segments. These modes are written as:

$$I_{1,2}(z) = \cos[2\pi(z \mp l/4)/l]. \tag{11}$$

Physically these modes correspond to current distributions of wavelength $\lambda = l$ centered at $\pm l/4$. The solution of the problem is then obtained by solving a matrix problem to determine the coefficients of the various modes in the expansion of the currents. For the frequencies considered in this study only the lowest order mode was required making the calculations extremely fast..

D. Scattering from a partially conducting cylinder.

In order to calculate the reflection from an array of plasma elements we make the physically reasonable assumption that (to first order) the induced current distribution in a partially-conducting plasma differs from that of a perfectly conducting scattering element only to the extent that the amplitude is different. In the limit of high conductivity the current distribution is the same as for a perfect conductor and in the limit of zero conductivity the current amplitude is zero.

The scattered electric field is directly proportional to the induced current on the scattering element. In turn, the reflectivity is thus directly proportional to the square of the induced current in the scattering element. Thus, to find the reflectivity of the plasma array, we determine the functional dependence of the induced squared current vs. the electromagnetic properties of the plasma and scale the reflectivity obtained for the perfectly conducting case accordingly.

In order to obtain the scaling function for the squared current we consider the following model problem. The problem of scattering is solved from an infinitely extended dielectric cylinder possessing the same dielectric properties as a partially-ionized, collisionless plasma. Assuming the

dielectric function for the plasma takes the following form:

$$\varepsilon(\omega) = 1 - \frac{\nu_p^2}{\nu^2}, \quad (12)$$

where, ν is the frequency of the incident electromagnetic wave, and ν_p is the plasma frequency defined by:

$$\nu_p = \frac{1}{2\pi}\sqrt{\frac{4\pi n e^2}{m}}, \quad (13)$$

where n is the density of ionized electrons, and e, and m, are the electron charge and mass respectively. A good conductor is characterized by the limit of large plasma frequency in comparison to the incident frequency. In the limit in which the plasma frequency vanishes, the plasma elements become completely transparent.

Now turning to the solution of the problem of scattering from a partially conducting cylinder. The conductivity, and thus the scattering properties of the cylinder are specified by the single parameter ν_p. Solving the wave equation for the electric field:

$$\nabla^2 E = \frac{1}{c^2}\frac{\partial^2 D}{\partial^2 t}, \quad (14)$$

subject to the boundary conditions that the tangential electric and magnetic fields must be continuous at the cylinder boundary. Considering the scattering resulting from the interaction of the cylinder with an incident plane wave of a single frequency. Therefore assuming all fields to have the harmonic time dependence:

$$e^{-i\omega t}, \quad (15)$$

where $\omega = 2\pi\nu$, is the angular frequency. We are adopting the physics convention for the time dependence. Personnel more familiar with the electrical engineering convention can easily convert all subsequent equations to that convention by making the substitution $i \to -j$.

Next we assume the standard approximation relating the displacement field to the electric field via the dielectric function:

$$D(\omega) = \varepsilon(\omega)E(\omega). \quad (16)$$

By imposing cylindrical symmetry, the wave equation takes the form of Bessel's equation:

$$\frac{\partial^2 E}{\partial^2 \rho} + \frac{1}{\rho}\frac{\partial E}{\partial \rho} + \frac{1}{\rho^2}\frac{\partial^2 E}{\partial \varphi^2} + \varepsilon k^2 E = 0, \quad (17)$$

where $k = \omega/c$, and (ρ, φ) are cylindrical polar coordinates. The general solution of this equation consists of linear combinations of products of Bessel functions with complex exponentials.The total field outside the cylinder consists of the incident plane wave plus a scattered field of the form:

$$E_{out} = e^{ik\rho\cos\varphi} + \sum_{m=-\infty}^{\infty} A_m H_m(k\rho) e^{im\varphi}, \quad (18)$$

where, A_m, is a coefficient to be determined and $H_m(k\rho) = J_m(k\rho) + iY_m(k\rho)$, is the Hankel function that corresponds to outgoing cylindrical scattered waves. The field inside the cylinder contains only Bessel functions of the first kind since it is required to be finite at the origin:

$$E_{in} = \sum_{m=-\infty}^{\infty} B_m J_m(k\rho\sqrt{\varepsilon}) e^{im\varphi}. \quad (19)$$

To facilitate the determination of the expansion coefficients A_m and B_m the incident plane wave is an expansion in Bessel[6] functions:

$$e^{ik\rho\cos\varphi} = \sum_{m=-\infty}^{\infty} i^m J_m(k\rho). \quad (20)$$

To enforce continuity of the electric field at the boundary of the cylinder:

$$E_{in}(\rho = a, \varphi) = E_{out}(\rho = a, \varphi), \quad (21)$$

where the cylinder is assumed to have radius a. The next boundary condition is obtained by imposing continuity of the magnetic field. From one of Maxwell's equations (Faraday's law) we obtain:

$$\overline{H} = -i(1/k)\nabla \times \overline{E}. \quad (22)$$

The electric field is assumed aligned with the cylinder axis (TM polarization). This is the only case of interest since the scattering of the TE wave is minimal. The tangential component of the magnetic field is thus:

$$H_\varphi = -i(1/k)\left[-\frac{\partial E_z}{\partial \rho}\right]. \quad (23)$$

By imposing the continuity of this field along with the continuity of the electric field, the following set of equations that determine the expansion coefficients is obtained:

$$i^m J_m(ka) + A_m H_m(ka) = B_m(ka\sqrt{\varepsilon}), \quad (24)$$

and,

$$i^m J'_m(ka) + A_m H'_m(ka) = B_m J'_m(ka\sqrt{\varepsilon})\sqrt{\varepsilon}, \quad (25)$$

where the primes on the Bessel and Hankel functions imply differentiation with respect to the argument.
These equations are easily solved for the expansion coefficients:

$$A_m = \frac{-i^m\left(\sqrt{\varepsilon}J_m(ka)J'_m(ka\sqrt{\varepsilon}) - J'_m(ka)J_m(ka\sqrt{\varepsilon})\right)}{\left(\sqrt{\varepsilon}H_m(ka)J'_m(ka\sqrt{\varepsilon}) - H'_m(ka)J_m(ka\sqrt{\varepsilon})\right)}, \quad (26)$$

and,

$$B_m = \frac{i^m(J_m(ka)H'_m(ka) - J'_m(ka)H_m(ka))}{H'_m(ka)J_m(ka\sqrt{\varepsilon}) - \sqrt{\varepsilon}H_m(ka)J'_m(ka\sqrt{\varepsilon})}. \quad (27)$$

Inspection of these coefficients shows that in the limit $\varepsilon \to 1$, (i.e. zero plasma frequency) we obtain $A_m \to 0,$ and $B_m \to i^m$. Thus in this limit, the scattered field vanishes and the field inside the cylinder simply becomes the incident field as expected.
The opposite limit of a perfectly conducting cylinder is also established fairly easily but requires somewhat more care. Consider first the field inside the cylinder, which must vanish in the perfectly conducting limit. A typical term in the expansion of the electric field inside the cylinder is of the form:

$$B_m J_m(k\rho\sqrt{\varepsilon}). \quad (28)$$

The perfect conductivity limit corresponds to taking the limit $\nu_p \to \infty,$ at fixed ν. In this limit $\varepsilon \to -\nu_p^2/\nu^2$, and thus $\sqrt{\varepsilon} \to i\nu_p/\nu$. For large imaginary argument the Bessel functions diverge exponentially. Therefore:

$$B_m J_m(k\rho\sqrt{\varepsilon}) \to O\left(\frac{\nu}{\nu_p}\right) \to 0. \quad (29)$$

Lastly we must establish that the tangential electric field just outside the cylinder vanishes in the perfect conductivity limit as expected. Using the fact that the Bessel functions diverge exponentially for large imaginary argument gives the following limit for the scattered wave expansion coefficient:

$$A_m \to \frac{-i^m J_m(ka)}{H_m(ka)}. \quad (30)$$

Thus a typical term in the expansion for the scattered wave, evaluated just outside the cylinder, has the following limit:

$$A_m H_m(ka) \to -i^m J_m(ka), \quad (31)$$

which exactly cancels the corresponding term in the expansion of the incident plane wave.
The scaling function defined below is used for the analysis of the scattering from a partially conducting cylinder to obtain a reasonable approximation to the scattering from a partially conducting plasma FSS array based on the computed results for a perfectly conducting array.
Proceeding based on the following observations/assumptions. (1) The reflectivity of the plasma FSS array is determined entirely in terms of the scattered field in contrast to the transmitted field which, depends on both the incident and scattered fields. (2) The shape of the current modes on the partially conducting (plasma) FSS array is the same as for the perfectly conducting array. (3) The only difference between the partially conducting and perfectly conducting arrays is the amplitude of the current modes.
Concluding that the reflectivity of the plasma FSS can be determined from that of the perfectly conducting array by scaling the reflectivity of the perfectly conducting array by some appropriately chosen scaling function. This conclusion follows from the fact that the reflectivity is directly proportional to the squared amplitude of the current distribution on the scattering elements.

E. Results

A case is presented: an array designed to have a well-defined reflection resonance near 1 GHz, (a band stop filter).
An array of plasma frequency selective surfaces was modeled. Similarly, we made the plasma FSS in the laboratory. Our theory and experiment were in close agreement. The response (reflection and transmission) of the plasma FSS is calculated in two stages. (1) The response for a perfectly conducting structure is given. (2) Then we scale the reflectivity by a function that depends on the incident frequency and the plasma frequency so as to account for the scattering properties of the plasma.

E. Switchable band stop filter

Consider an plasma FSS dipole array. Each scattering element is assumed to be $15cm$ in length, $1cm$ in diameter. The vertical separation is taken to be $18cm,$ while the lateral separation is taken to be $10cm.$ The array elements are the vertically aligned rectangular regions. For convenience of analysis, the array is assumed to extend infinitely in the plane.

The results for the perfectly conducting case along with those for several values of the plasma frequency are presented in Fig. 1. A well-defined reflectivity resonance exists at 1GHz. This result indicates that appreciable reflection occurs only for plasma frequencies above 2.5GHz. The results of Fig. 1 illustrate the essence of the plasma FSS: a highly reflective The results for the perfectly conducting case along with those for several values of the plasma frequency are presented in Fig. 2. A well-defined reflectivity resonance exists at 1GHz. This result indicates that appreciable reflection occurs only for plasma frequencies above 2.5GHz.

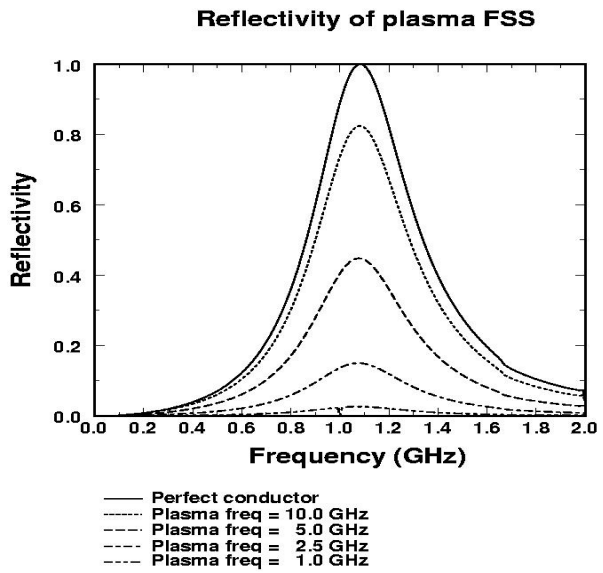

Figure 1. Calculated reflectivity of a dipole, plasma FSS array for several values of the plasma frequency.

III. PLASMA FSS MEASURMENTS

The superposition of the experimental and theoretical work is given in Fig. 2 shows good agreement. Differences are due mainly that the theoretical plot was an infinite array and the experimental plot was finite. The peak resonance in the theoretical and experimental plots was very close, and the sub peaks in the experimental is due to the finite size of the array.

Figure 2. Experimental and theoretical plots of plasma FSS superimposed. Plasma tubes were 10.16 cm inches long and 12.7 cm inches long with metal ends included., 5.08 cm apart horizontally, and 2.54 cm apart vertically.

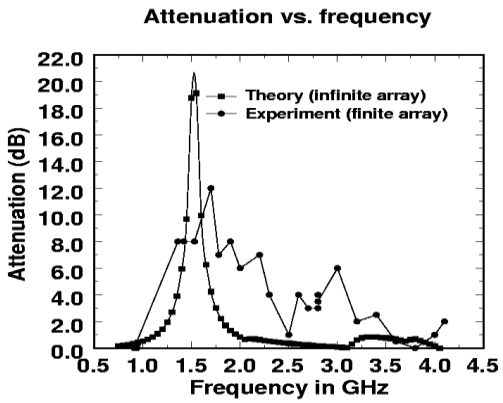

Fig. 3 is an example of a simple plasma FSS dipole configuration.

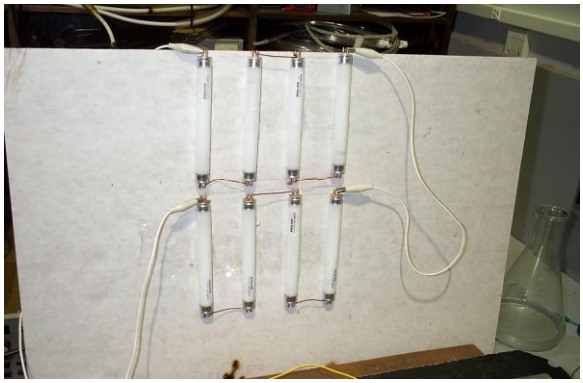

Figure 3. Example of an experimental plasma FSS

IV. CONCLUSIONS

The plasma FSS can shield antennas, electronics and radar systems in a tunable way. If no shielding is needed, turning the plasmas off causes the shield to cease to exist. Plasma FSS allow users to filter out any undesirable radiation, but at the same time enabling operations outside that band in a reconfigurable instead of a fixed way. The potential for technology transfer is significant since the plasma FSS can be tuned to filter out unwanted radiation from commercial products or tuned to filter electromagnetic emissions to meet FCC EMC requirements. For more information on plasma frequency selective surfaces see chapter 8 of Anderson [2].

REFERENCES

[1] T. Anderson, I. Alexeff, "Plasma frequency selective surfaces", IEEE Transactions on Plasma Science, Vol. 35, issue. 2, pp. 407-415, April 2007

[2] T. Anderson, Plasma Antennas, Artech House, pp. 113-127, July 2011

[3] B. A. Munk, Frequency Selective Surfaces**,** Wiley Interscience, 2000.

[4] I. Alexeff, T. Anderson, "Experimental and theoretical results with plasma antennas", IEEE Transactions on Plasma Science, Vol. 34, Issue 2, April 2006.

[5] I. Alexeff., T. Anderson, "Recent results of plasma antennas" , Physics of Plasmas, Volume 15, Issue 5, pp. 057104-057104-4, May 2008.

[6] O. Sakai, K. Tachibana, "Plasmas as metamaterials: a review", Plasma Sources Sci. Technol. 21, pp 013001-013019, 31January,20